

# The flux of ultra-high-energy cosmic rays along the supergalactic plane measured at the Pierre Auger Observatory

THE PIERRE AUGER COLLABORATION

Submitted to ApJ

## ABSTRACT

Ultra-high-energy cosmic rays are known to be mainly of extragalactic origin, and their propagation is limited by energy losses, so their arrival directions are expected to correlate with the large-scale structure of the local Universe. In this work, we investigate the possible presence of intermediate-scale excesses in the flux of the most energetic cosmic rays from the direction of the supergalactic plane region using events with energies above 20 EeV recorded with the surface detector array of the Pierre Auger Observatory up to 31 December 2022, with a total exposure of 135,000 km<sup>2</sup> sr yr. The strongest indication for an excess that we find, with a post-trial significance of 3.1 $\sigma$ , is in the Centaurus region, as in our previous reports, and it extends down to lower energies than previously studied. We do not find any strong hints of excesses from any other region of the supergalactic plane at the same angular scale. In particular, our results do not confirm the reports by the Telescope Array collaboration of excesses from two regions in the Northern Hemisphere at the edge of the field of view of the Pierre Auger Observatory. With a comparable exposure, our results in those regions are in good agreement with the expectations from an isotropic distribution.

*Keywords:* Cosmic rays (329), Ultra-high-energy cosmic radiation (1733), Cosmic anisotropy (316)

## 1. INTRODUCTION

The flux of ultra-high-energy cosmic rays (UHECRs), atomic nuclei mainly of extragalactic origin reaching the Earth with energies  $E \geq 1 \text{ EeV} = 10^{18} \text{ eV} \approx 0.16 \text{ J}$  each, is remarkably close to being the same from all directions in the sky, with the exception of a dipole moment in the celestial distribution of cosmic rays with  $E \geq 8 \text{ EeV}$  (Pierre Auger Collaboration 2017, 2018a, 2020a) towards a direction  $\sim 115^\circ$  away from the Galactic Center, with an amplitude of around 7% and growing roughly linearly with energy. No anisotropies on intermediate or smaller angular scales have been conclusively discovered yet in data collected at either the Pierre Auger Observatory or the Telescope Array (TA), the two largest cosmic-ray detector arrays in the world (covering 3000 km<sup>2</sup> and 700 km<sup>2</sup> respectively), located in the Southern and Northern Hemisphere (latitudes  $-35^\circ 2$

and  $+39^\circ 3$ ), respectively. On the other hand, a few indications with statistical significances ranging from 3.0 $\sigma$  to 4.6 $\sigma$  of such anisotropies in the flux of cosmic rays with more than a few tens of EeV have been reported. An excess of events in data from the Pierre Auger Observatory from a circular region on the celestial sphere (a “top-hat” window) centered on the Centaurus A (Cen A) radio galaxy, first reported in Pierre Auger Collaboration (2010), has reached a post-trial significance of 4.0 $\sigma$  (Pierre Auger Collaboration 2023). A correlation with the positions of nearby starburst galaxies first reported in Pierre Auger Collaboration (2018b), to which the main contributor is the NGC4945 galaxy in the aforementioned Cen A region, has reached 3.8 $\sigma$  post-trial as of the last update (Pierre Auger Collaboration 2023). An analogous study combining data from both the Pierre Auger Observatory and the Telescope Array has reached 4.6 $\sigma$  post-trial (Pierre Auger Collaboration & Telescope Array Collaboration 2023b). Finally, the so-called “TA hotspot” (Telescope Array Collaboration 2014) and a new excess from another region

of the Northern Hemisphere (Telescope Array Collaboration 2021b) in TA data have post-trial significances around  $3\sigma$  as of their last update (Telescope Array Collaboration 2023). All these regions where indications of excesses have been reported intersect the supergalactic plane (SGP), a great circle in the sky along which extragalactic matter within  $\mathcal{O}(10^2 \text{ Mpc})$  tends to be concentrated. The Local Sheet, a structure comprising nearly all bright galaxies within 6 Mpc (McCall 2014), is also remarkably aligned with the SGP. Hence, a concentration of the flux of the highest-energy cosmic rays along this plane would not be completely unexpected, given that propagation lengths at the highest energies are limited to a few hundred Mpc—or even less, in the case of intermediate-mass nuclei (Allard 2012). On the other hand, UHECRs can undergo substantial deflections by Galactic and possibly intergalactic magnetic fields (Unger & Farrar 2023; Pshirkov et al. 2013; Alves Batista et al. 2017), preventing a one-to-one interpretation of arrival directions in terms of source positions.

Here, we leverage the intermediate angular scale of the aforementioned excess from the region reported in data from the Pierre Auger Observatory. As of the last update (Pierre Auger Collaboration 2023), the maximum statistical significance for a top-hat window was achieved with an energy threshold of  $E_{\min} = 38 \text{ EeV}$  and a window radius of  $\Psi = 27^\circ$ , whether the center of the window was constrained to be the position of Cen A or also scanned to avoid any assumption on the possible source location. In this work, we study whether other excesses with similar characteristics are present in different regions along the SGP, and/or at lower energies than previously studied. A search for excesses of events in bands centered around the SGP found no statistically significant result ( $p = 0.13$  post-trial, Pierre Auger Collaboration 2022, section 3.3), but a band in latitude may not capture an excess concentrated in a limited range of supergalactic longitude, hence in this work we consider top-hat windows intersecting the SGP instead.

## 2. THE DATASET

We use the same dataset used in our last update on arrival directions (Pierre Auger Collaboration 2023) for searches for medium-scale anisotropies, namely events recorded using the surface detector (SD) array of the Pierre Auger Observatory in the years from 2004 to 2022 inclusive, except that here we lower the energy threshold from 32 EeV to 20 EeV. The selection criteria and reconstruction procedures are the same as used for the published dataset of Pierre Auger Collaboration (2022). Namely, we use all “vertical” events (with zenith an-

gles  $\theta < 60^\circ$ ) in which the SD station with the largest signal is surrounded by at least four active stations and the reconstructed shower core is within an isosceles triangle of active stations, and all “inclined” events (with  $60^\circ \leq \theta < 80^\circ$ ) in which the station closest to the reconstructed core position is surrounded by at least five active stations. The energies of these events are reconstructed with a total systematic uncertainty  $\sim 14\%$  and resolution  $\sim 7\%$ , and their arrival directions with a resolution  $< 1^\circ$ . Compared to the published dataset (Pierre Auger Collaboration 2022), here we also use events detected in the years 2021 and 2022 and events with energies  $20 \text{ EeV} \leq E < 32 \text{ EeV}$  over the entire time period. As regards the last two years, only events detected by the parts of the array that had not yet undergone the AugerPrime upgrade (Pierre Auger Collaboration 2016) are used. The total exposure of this dataset is  $135,000 \text{ km}^2 \text{ sr yr}$ .

As in Pierre Auger Collaboration (2022, 2023), the exposures to vertical and inclined events are rescaled so as to be proportional to the number of events in each zenith angle range (respectively 6896 and 1936 above 20 EeV). We have verified that, compared with the use of “nominal” vertical and inclined exposures (respectively 106,000 and 29,100  $\text{km}^2 \text{ sr yr}$ ), this affects the resulting computed flux in circular regions of the Southern sky by  $\lesssim 3\%$  and the significance of excesses in these regions by  $\lesssim 0.1\sigma$ . By combining both zenith angle ranges ( $0^\circ \leq \theta < 80^\circ$ ), the field of view (FoV) of the SD array covers all declinations  $-90^\circ \leq \delta < +44^\circ 8'$ .

## 3. ANALYSIS METHOD

In this work, for each of six different energy thresholds,  $E_{\min} = 20, 25, 32, 40, 50, 63 \text{ EeV}$  (i.e.,  $10^{19.3, 19.4, \dots, 19.8} \text{ eV}$  rounded to the nearest EeV), we consider all top-hat windows with radius  $\Psi = 27^\circ$  (the maximum-significance radius in Pierre Auger Collaboration 2023) centered on the positions on a HEALPix<sup>1</sup> grid (Górski et al. 2005) with  $N_{\text{side}} = 2^6$  (resolution  $\approx 0.9^\circ$ ) simultaneously meeting two criteria: first, we require that the SGP intersect the window, i.e., that the supergalactic latitude  $B$  of the window center satisfy  $-\Psi \leq B \leq \Psi$ ; and second, as in our previous works, in order to have reasonably large statistics we require that the center of the window be inside the FoV of the Observatory, i.e., that the declination of the window

<sup>1</sup> <https://healpix.sourceforge.io/>

center satisfy  $\delta < +44^\circ.8$ .<sup>2</sup> For each such window, we counted the numbers  $N_{\text{in}}, N_{\text{out}}$  of events in our dataset with  $E \geq E_{\text{min}}$  respectively inside the window and in the rest of the FoV, and computed the exposures  $\mathcal{E}_{\text{in}}, \mathcal{E}_{\text{out}}$  by numerically integrating the expression in Sommers (2001, section 2). From these, we computed the background number of events  $N_{\text{bg}}$  as  $N_{\text{out}}\mathcal{E}_{\text{in}}/\mathcal{E}_{\text{out}}$ , and the flux ratio  $\Phi_{\text{in}}/\Phi_{\text{out}}$  as  $N_{\text{in}}/N_{\text{bg}}$  (see below).

### 3.1. Binomial probability, likelihood and upper limit

For a given value of the ratio  $\Phi_{\text{in}}/\Phi_{\text{out}}$  between the flux inside the window and that in the rest of the FoV (the isotropic null hypothesis being  $\Phi_{\text{in}}/\Phi_{\text{out}} = 1$ ) and total number  $N_{\text{tot}} = N_{\text{in}} + N_{\text{out}}$  of events above the energy threshold, the probability to observe exactly  $N_{\text{in}}$  events inside the window is

$$P\left(N_{\text{in}} \mid N_{\text{tot}}, \frac{\Phi_{\text{in}}}{\Phi_{\text{out}}}\right) = \binom{N_{\text{tot}}}{N_{\text{in}}} p^{N_{\text{in}}} (1-p)^{N_{\text{tot}}-N_{\text{in}}}, \quad (1)$$

where

$$p = \frac{\Phi_{\text{in}}\mathcal{E}_{\text{in}}}{\Phi_{\text{in}}\mathcal{E}_{\text{in}} + \Phi_{\text{out}}\mathcal{E}_{\text{out}}} \quad (2)$$

is the probability for each event to fall within the window. This probability as a function of  $\Phi_{\text{in}}/\Phi_{\text{out}}$  for a fixed  $N_{\text{in}}, N_{\text{out}}$  defines a likelihood function,

$$L(\Phi_{\text{in}}/\Phi_{\text{out}}) = P(N_{\text{in}} \mid N_{\text{tot}}, \Phi_{\text{in}}/\Phi_{\text{out}}), \quad (3)$$

which achieves its maximum at  $\Phi_{\text{in}}/\Phi_{\text{out}} = \frac{N_{\text{in}}/\mathcal{E}_{\text{in}}}{N_{\text{out}}/\mathcal{E}_{\text{out}}} = N_{\text{in}}/N_{\text{bg}}$ .

If we define the deviance (generalized  $\chi^2$ , here with one degree of freedom) as

$$\begin{aligned} D(\Phi_{\text{in}}/\Phi_{\text{out}}) &= -2 \ln \frac{L(\Phi_{\text{in}}/\Phi_{\text{out}})}{\max_{\Phi_{\text{in}}/\Phi_{\text{out}}} L(\Phi_{\text{in}}/\Phi_{\text{out}})} \\ &= -2 \ln \frac{L(\Phi_{\text{in}}/\Phi_{\text{out}})}{L(N_{\text{in}}/N_{\text{bg}})}, \end{aligned} \quad (4)$$

then  $\pm\sqrt{D(\Phi_{\text{in}}/\Phi_{\text{out}})}$  is the number of standard deviations at which the dataset disfavors a given value of  $\Phi_{\text{in}}/\Phi_{\text{out}}$  with respect to the value  $N_{\text{in}}/N_{\text{bg}}$ ; in particular,  $\pm\sqrt{D(\Phi_{\text{in}}/\Phi_{\text{out}} = 1)}$  equals the local Li–Ma significance  $Z_{\text{LM}}$  (Li & Ma 1983).<sup>3</sup> The statistical uncertainties in  $\Phi_{\text{in}}/\Phi_{\text{out}}$  we report in the tables are the  $\pm 1\sigma$  intervals defined this way.

<sup>2</sup> Note that this is slightly more conservative than the recommendation by Li & Ma (1983) that  $N_{\text{in}} \gtrsim 10$  and  $N_{\text{out}} \gtrsim 10$  when using the lowest of the energy thresholds we use here but slightly less conservative using the highest thresholds, i.e., some of the windows with centers closest to the edge of the FoV have  $N_{\text{in}} \lesssim 10$  when using the highest thresholds.

<sup>3</sup> The sign is + or – depending on whether  $\Phi_{\text{in}}/\Phi_{\text{out}}$  is larger or smaller than the maximum-likelihood value  $N_{\text{in}}/N_{\text{bg}}$ .

Finally, we define the frequentist 99% confidence level upper limit to  $\Phi_{\text{in}}/\Phi_{\text{out}}$  as the  $\Phi_{\text{in}}/\Phi_{\text{out}}$  value such that

$$\sum_{n=N_{\text{in}}+1}^{N_{\text{tot}}} P(n \mid N_{\text{tot}}, \Phi_{\text{in}}/\Phi_{\text{out}}) = 0.01; \quad (5)$$

in the cases we report, this agrees with the value such that  $\sqrt{D(\Phi_{\text{in}}/\Phi_{\text{out}})} = 2.33$  to within a few percent.

## 4. RESULTS

The local Li–Ma significance  $Z_{\text{LM}}$  as a function of the position of the window center in supergalactic coordinates ( $L, B$ ) is shown in Figure 1, and the information about the window with the highest  $Z_{\text{LM}}$  for each  $E_{\text{min}}$  is listed in Table 1. We also search for the highest  $Z_{\text{LM}}$  among windows which do not overlap with the global maximum one (distance between centers  $> 2\Psi$ ). In Figure 2, we show the flux ratio  $\Phi_{\text{in}}/\Phi_{\text{out}}$  computed as  $N_{\text{in}}/N_{\text{bg}}$  as a function of the position of the window center.

### 4.1. Indication of an excess in the Centaurus region

As shown in the left part of Table 1 and by the solid circles in Figure 1, with all energy thresholds the most significant excess is the previously reported one in the Centaurus region. Its position is remarkably stable at least over a range of energy thresholds spanning half an order of magnitude (and of cumulative UHECR flux values spanning one and a half order of magnitude), with no discernible change in the maximum-significance window center. On the other hand, the strength  $\Phi_{\text{in}}/\Phi_{\text{out}}$  of the excess does grow with the energy threshold, implying that the particles making up the excess have a different energy spectrum than the background, with a slower decrease with energy. By studying the number of events in this region in separate energy bins (see Appendix A for details), we find that the excess has a spectral index  $\gamma = 2.6 \pm 0.3$ . For comparison, the overall spectrum in our FoV (Pierre Auger Collaboration 2020b, with stricter quality cuts and a different reconstruction) has  $\gamma = 3.05 \pm 0.05 \pm 0.10$  below  $(46 \pm 3 \pm 6)$  EeV and  $\gamma = 5.1 \pm 0.3 \pm 0.1$  above, where the first uncertainty is statistical and the second is systematic.

The local significance of  $+5.2\sigma$  we find in the Centaurus region using the lowest energy threshold is exceeded for at least one of the window positions and energy thresholds in 912 out of  $10^6$  isotropic simulations, corresponding to a  $3.1\sigma$  post-trial significance.

### 4.2. Study of Telescope Array reported excess regions

As shown in the right part of Table 1 and by the dashed circles in Figure 1, the local significances of ex-

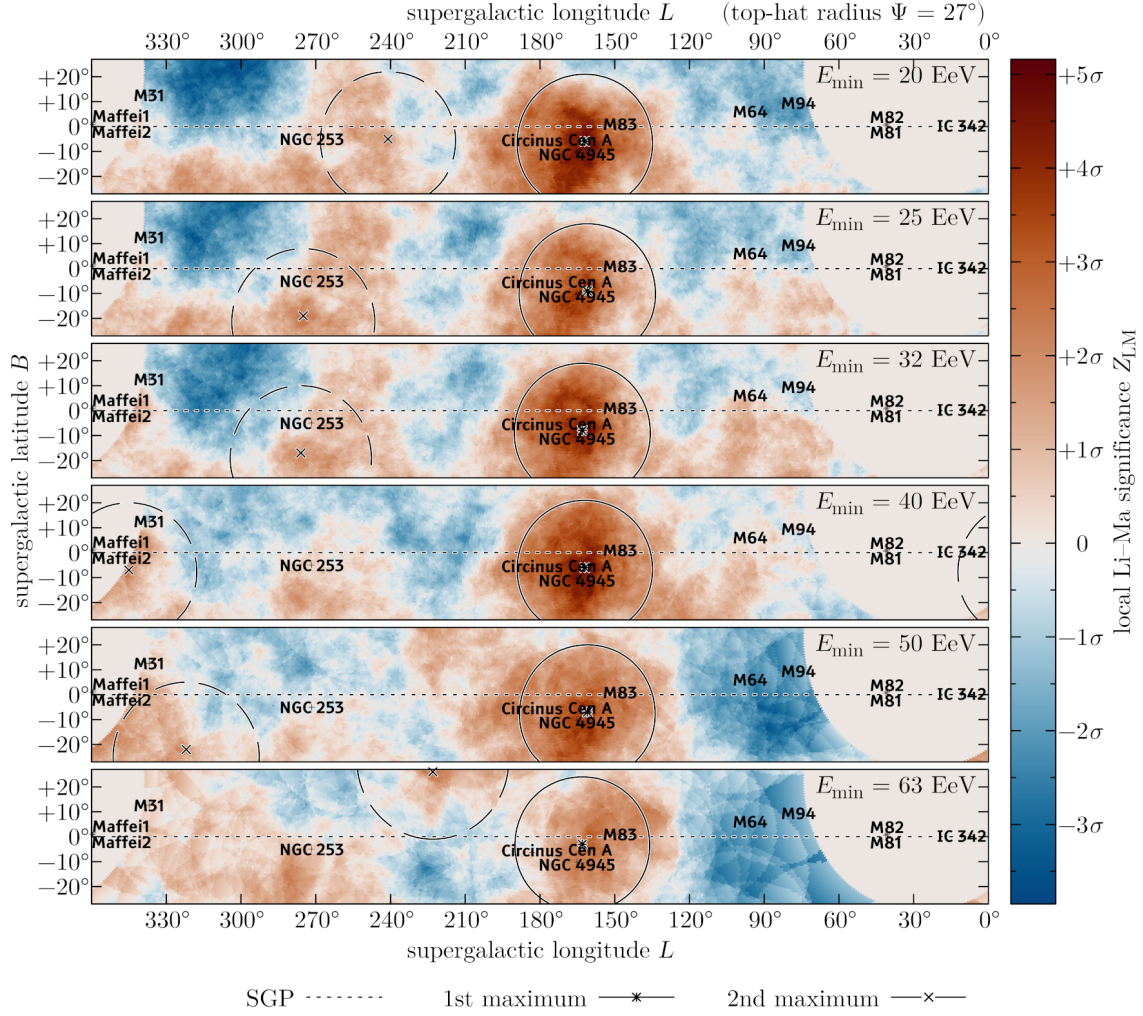


**Figure 1.** Local Li–Ma significance  $Z_{LM}$  of excesses over the isotropic expectation as a function of the window center position. The  $Z_{LM}$  in windows whose center lies outside the FoV of the Observatory was not computed (shown as the gray disk wrapping around the left and right edges of each panel; see also Figure 3). In each panel, the energy threshold used is written in the upper right corner. The solid circle is the window position with the highest  $Z_{LM}$  in the whole strip; the dashed one is that with the highest  $Z_{LM}$  excluding those overlapping with the solid one. Labels indicate the position of Council of Giants galaxies (McCall 2014) for reference only; they are not taken into account in the analysis in any way.

**Table 1.** Information about the maximum-significance excesses found along the SGP

$E_{\min}$	$N_{\text{tot}}$	1st maximum								2nd maximum							
		$L$	$B$	$\frac{\varepsilon_{\text{in}}}{\varepsilon_{\text{tot}}}$	$N_{\text{bg}}$	$N_{\text{in}}$	$\frac{\Phi_{\text{in}}}{\Phi_{\text{out}}}$	$Z_{LM}$	99% U.L.	$L$	$B$	$\frac{\varepsilon_{\text{in}}}{\varepsilon_{\text{tot}}}$	$N_{\text{bg}}$	$N_{\text{in}}$	$\frac{\Phi_{\text{in}}}{\Phi_{\text{out}}}$	$Z_{LM}$	99% U.L.
20 EeV	8832	162°	−6°	9.56%	829.	990	$1.19^{+0.04}_{-0.04}$	+5.2σ	1.29	241°	−5°	10.27%	900.	971	$1.08^{+0.04}_{-0.04}$	+2.2σ	1.17
25 EeV	5380	161°	−9°	9.56%	504.	608	$1.21^{+0.05}_{-0.05}$	+4.2σ	1.33	275°	−19°	8.00%	426.	482	$1.13^{+0.05}_{-0.05}$	+2.6σ	1.26
32 EeV	2936	163°	−8°	9.68%	276.	363	$1.32^{+0.08}_{-0.07}$	+4.7σ	1.50	276°	−17°	7.89%	229.	264	$1.15^{+0.08}_{-0.07}$	+2.2σ	1.34
40 EeV	1533	162°	−6°	9.56%	140.	208	$1.49^{+0.11}_{-0.11}$	+5.1σ	1.77	345°	−7°	1.00%	15.2	26	$1.71^{+0.36}_{-0.32}$	+2.5σ	2.68
50 EeV	713	161°	−7°	9.56%	64.4	103	$1.60^{+0.18}_{-0.16}$	+4.2σ	2.05	322°	−22°	3.69%	25.9	39	$1.51^{+0.26}_{-0.23}$	+2.4σ	2.20
63 EeV	295	163°	−3°	9.56%	26.3	46	$1.75^{+0.30}_{-0.26}$	+3.3σ	2.54	223°	+26°	9.56%	26.7	42	$1.57^{+0.28}_{-0.25}$	+2.6σ	2.31

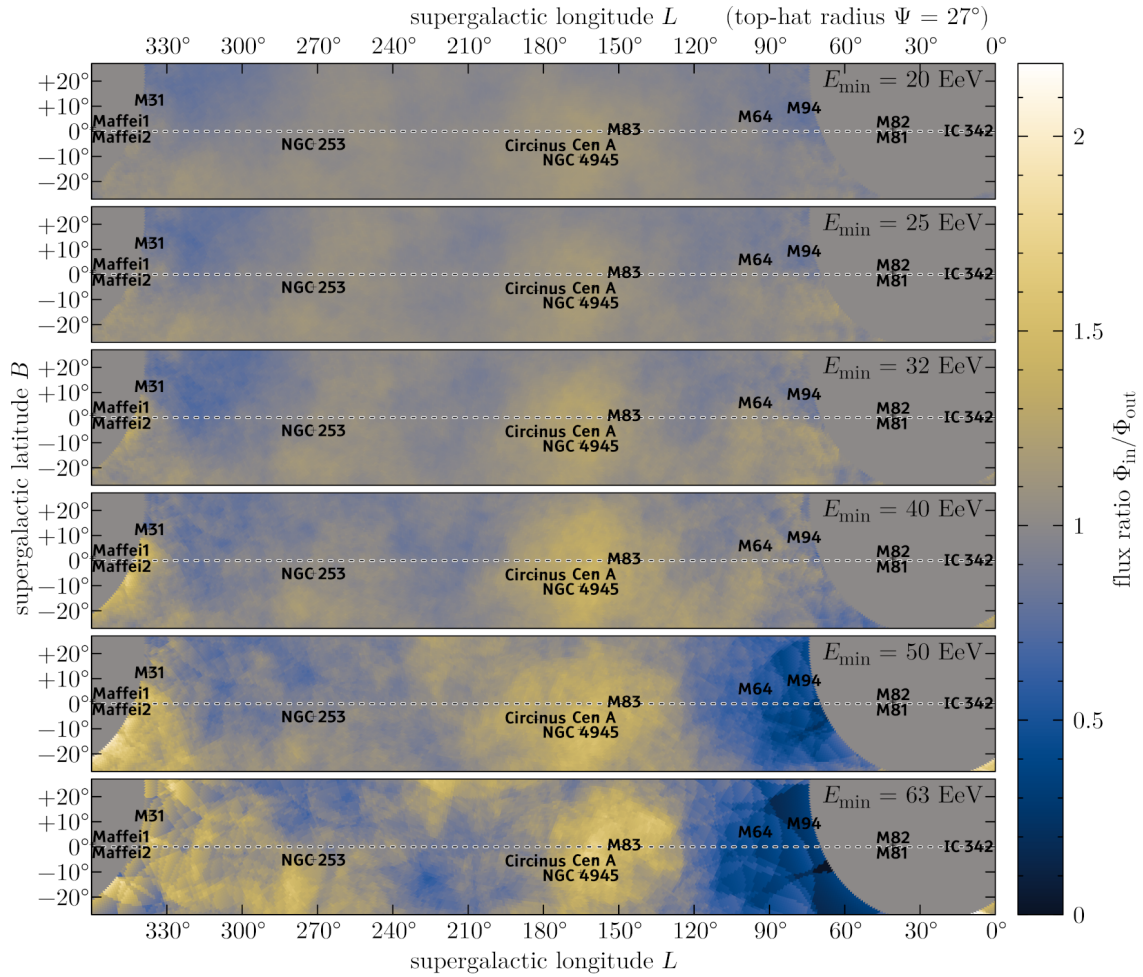


**Figure 2.** The maximum-likelihood value of the ratio  $\Phi_{\text{in}}/\Phi_{\text{out}}$ , i.e.,  $N_{\text{in}}/N_{\text{bg}}$ , as a function of the window center position

cesses in windows not overlapping with the maximum-significance one are below  $2.7\sigma$  for all the energy thresholds we tested. As shown in [Appendix B](#), this sets stringent upper limits on the flux, except very close to the edge of our FoV. The non-observation of other excesses at this angular scale appears to contradict the reports by the TA collaboration of an excess of cosmic rays with energies  $E \geq 57\text{EeV}$  from a particular top-hat window (hereafter “TA hotspot”) in the Northern Hemisphere ([Telescope Array Collaboration 2014](#)) and later of a weaker excess of events with  $E \geq 10^{19.4,19.5,19.6}\text{eV}$  from a different window ([Telescope Array Collaboration 2021b](#)), both shown in [Figure 3](#). Despite global statistical significances of only  $\sim 3\sigma$ , such reports have already spurred several attempted phenomenological interpretations (e.g., [Neronov et al. 2023](#); [Plotko et al. 2023](#); [Anchordoqui 2023](#)).

Both of these regions are in the part of the sky studied in this work (see [Figure 3](#)), but as shown in [Figure 1](#) we do not find any excesses at these positions when using comparable energy thresholds. The second most significant excess visible in the fourth panel of [Figure 2](#) at  $L \approx 345^\circ$  is centered around  $20^\circ$  further east than the TA new excess—whereas the statistical uncertainty on the window position is of the order of  $\Psi/\sqrt{N_{\text{in}} - N_{\text{bg}}} \sim 8^\circ$  in this case. The one visible in the second and third panels of [Figure 2](#) at  $L \approx 65^\circ$  is replaced by a deficit in the last two panels—the opposite of the energy dependence of [Telescope Array Collaboration 2018a](#), which reported a deficit of events with  $10^{19.2}\text{eV} \leq E < 10^{19.75}\text{eV}$  and an excess with  $E \geq 10^{19.75}\text{eV}$ .

To find out what we could have expected to observe in our data given those reports from TA, after correcting the energy thresholds for the known mismatch between the energy scales of the two observatories ([Pierre Auger Collaboration & Telescope Array Collaboration 2023b](#), eq. (1)), we computed the distribution of the number  $N_{\text{in}}$  of events in our dataset expected in each of these windows based on (i) isotropy ( $\Phi_{\text{in}}/\Phi_{\text{out}} = 1$ ), (ii) the TA value of  $\Phi_{\text{in}}/\Phi_{\text{out}}$  that can be computed from their numbers of events  $N_{\text{in}}, N_{\text{tot}}$  as reported in their last update ([Telescope Array Collaboration 2023](#)), or (iii) the marginal distribution of  $\Phi_{\text{in}}/\Phi_{\text{out}}$  over TA statistical uncertainties. As we show in [Figure 4](#), in each case we find that based on the TA result we would expect on average a local Li–Ma significance in our data of the order of  $4\sigma$ , comparable to the TA value—since we have accumulated comparable amounts of exposure in

these windows, as shown by the  $N_{\text{bg}}$  values<sup>4</sup> in [Table 2](#). (The smaller fraction of the exposure of the Pierre Auger Observatory than of the Telescope Array within these northern regions is compensated by the larger total exposure of the former.) Instead, what we actually obtain is always  $-0.7\sigma \lesssim Z_{\text{LM}} < +0.2\sigma$ , in excellent agreement with the isotropic null hypothesis. In all cases, there exist possible values of  $\Phi_{\text{in}}/\Phi_{\text{out}}$  which would be compatible with both the 99% CL lower limit from TA data and the 99% CL upper limit from our data, e.g.,  $1.60 < \Phi_{\text{in}}/\Phi_{\text{out}} < 1.76$  in (a).

To take into account the possibility that [Pierre Auger Collaboration & Telescope Array Collaboration \(2023b, eq. \(1\)\)](#) under- or overestimates the energy on the Pierre Auger Observatory scale corresponding to a given energy on the Telescope Array because of statistical and systematic uncertainties in the fit, we also computed  $\Phi_{\text{in}}/\Phi_{\text{out}}$  and  $Z_{\text{LM}}$  values with different energy thresholds, finding that no other choice of threshold yields significances comparable to what we would expect based on the TA results, either ([Figure 5](#)).

A limitation of this study is that the likelihood in [Equation 3](#) implicitly assumes a constant UHECR flux  $\Phi_{\text{in}}$  inside the window being considered and a constant flux  $\Phi_{\text{out}}$  outside. Whereas the directional exposure of the Telescope Array is roughly uniform within the windows shown in [Figure 3](#), that of the Pierre Auger Observatory steeply decreases with increasing declination (and even vanishes in part of the windows). Hence, a flux excess more concentrated in the northern than in the southern part of a window would on average be underestimated when using data from the Auger Observatory. On the other hand, it should be noted that the TA window positions were chosen to maximize the statistical significance of the excesses using TA data, so, if a flux excess had been larger in the northern than in the southern part of such a window, the maximum-significance window position would presumably have been further north. Similar considerations could apply to a declination dependence of the flux outside the window being considered, but in [Pierre Auger Collaboration \(2020b\)](#) we found that the flux of UHECRs does not appreciably vary with declination within our FoV other than the dipole mentioned in [section 1](#), and the declination dependence claimed in [Telescope Ar-](#)

<sup>4</sup> We cannot compute the absolute exposure of TA within each window (in  $\text{km}^2\text{sr yr}$ ) to directly compare it with ours, as [Telescope Array Collaboration \(2023\)](#) did not report the total exposure of the dataset. ([Pierre Auger Collaboration & Telescope Array Collaboration 2023b](#) did, but a different TA dataset with stricter selection criteria was used there.)

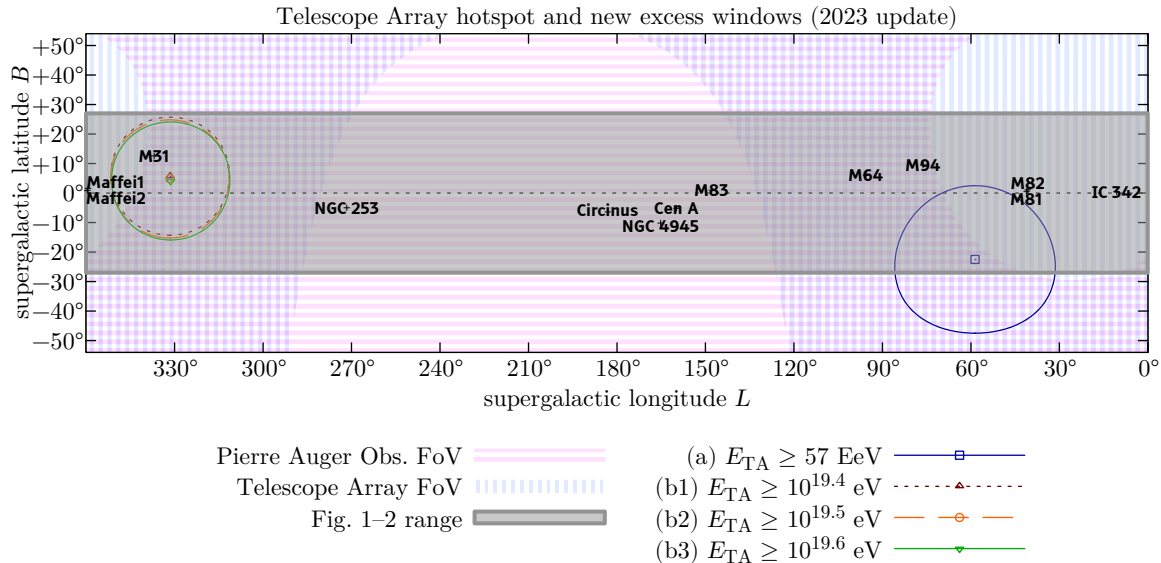


**Figure 3.** The windows in which the TA collaboration reported excesses of events, as of their latest update (*Telescope Array Collaboration 2023*), compared to the FoV of the Pierre Auger Observatory and of the Telescope Array

**Table 2.** The excesses reported by TA in the windows shown in *Figure 3*, as of their latest update (*Telescope Array Collaboration 2023*), and the corresponding results in our data. The  $E_{\min}$  values are converted from the TA energy scale to ours using *Pierre Auger Collaboration & Telescope Array Collaboration (2023b, eq. (1))*. Some of the TA values of  $N_{\text{bg}}$ ,  $\Phi_{\text{in}}/\Phi_{\text{out}}$  and/or  $Z_{\text{LM}}$  shown here differ by up to a few percent from those reported in *Telescope Array Collaboration (2023)*, presumably because in that work  $\mathcal{E}_{\text{in}}/\mathcal{E}_{\text{tot}}$  was estimated from a Monte Carlo simulation with 100,000 events (of which  $\mathcal{O}(10^4)$  within the window, hence with fluctuations  $\sim 1\%$  in  $\mathcal{E}_{\text{in}}$ ), whereas here we computed it by numerically integrating the expression in *Sommers (2001, section 2)* over a HEALPix grid with  $N_{\text{side}} = 2^{10}$  (resolution  $\approx 0.06^\circ$ ). For the TA results, we computed the frequentist 99% CL lower limit to  $\Phi_{\text{in}}/\Phi_{\text{out}}$  defined analogously to (5) by  $\sum_{n=0}^{N_{\text{in}}-1} P(n|N_{\text{tot}}, \Phi_{\text{in}}/\Phi_{\text{out}}) = 0.01$ . Note that the TA post-trial significances were computed under the assumption that only excesses near the center of a presumed emitting structure (the Perseus–Pisces Supercluster) had been searched for.

	Telescope Array ( <i>Telescope Array Collaboration 2023</i> )									Pierre Auger Observatory (this work)							
	$E_{\min}$	$N_{\text{tot}}$	$\frac{\mathcal{E}_{\text{in}}}{\mathcal{E}_{\text{tot}}}$	$N_{\text{bg}}$	$N_{\text{in}}$	$\frac{\Phi_{\text{in}}}{\Phi_{\text{out}}}$	$Z_{\text{LM}}$	99% L.L.	post-trial	$E_{\min}$	$N_{\text{tot}}$	$\frac{\mathcal{E}_{\text{in}}}{\mathcal{E}_{\text{tot}}}$	$N_{\text{bg}}$	$N_{\text{in}}$	$\frac{\Phi_{\text{in}}}{\Phi_{\text{out}}}$	$Z_{\text{LM}}$	99% U.L.
(a)	57 EeV	216	9.47%	18.0	44	$2.44^{+0.44}_{-0.39}$	$+4.8\sigma$	1.60	$2.8\sigma$	44.6 EeV	1074	1.00%	10.7	9	$0.84^{+0.31}_{-0.25}$	$-0.5\sigma$	1.76
(b1)	$10^{19.4}$ eV	1125	5.88%	64.0	101	$1.58^{+0.17}_{-0.16}$	$+4.1\sigma$	1.22	$3.3\sigma$	20.5 EeV	8374	0.84%	70.1	65	$0.93^{+0.12}_{-0.11}$	$-0.6\sigma$	1.23
(b2)	$10^{19.5}$ eV	728	5.87%	41.1	70	$1.70^{+0.22}_{-0.20}$	$+4.0\sigma$	1.25	$3.2\sigma$	25.5 EeV	5156	0.84%	43.5	39	$0.90^{+0.15}_{-0.14}$	$-0.7\sigma$	1.29
(b3)	$10^{19.6}$ eV	441	5.84%	24.6	45	$1.83^{+0.31}_{-0.27}$	$+3.6\sigma$	1.23	$3.0\sigma$	31.7 EeV	2990	0.87%	26.0	27	$1.04^{+0.21}_{-0.19}$	$+0.2\sigma$	1.61

ray Collaboration (2018b), if anything, would make the Telescope Array overestimate and the Auger Observatory underestimate  $\Phi_{\text{out}}$ , going in the opposite direction than what would explain away the difference between the  $\Phi_{\text{in}}/\Phi_{\text{out}}$  values from the two datasets.

## 5. DISCUSSION AND CONCLUSIONS

We have confirmed our previous finding (*Pierre Auger Collaboration 2023*, with  $4.0\sigma$  post-trial there) that the statistically most significant excess of UHECRs along the SGP is from the Centaurus region, though still not at the discovery level with the current statistics (post-trial significance  $3.1\sigma$  in this work), and we have further found that this excess extends to lower energies than

previously studied (down to 20 EeV), with no appreciable dependence of its position on the energy threshold chosen. One possible explanation for this lack of energy dependence (other than the absence of sizable coherent magnetic deflections) could be an approximately constant magnetic rigidity  $R = E/Z$  of the particles making up this excess, i.e., an increasingly heavy mass composition such that their atomic numbers  $Z$  are proportional to their energy. It was already predicted by *Lemoine & Waxman (2009)* that in the case of a mixed composition anisotropies at high energies should be expected to correspond to anisotropies of lighter nuclei at lower energies, but in *Pierre Auger Collaboration (2011)* we had failed to find any such indication possibly due to

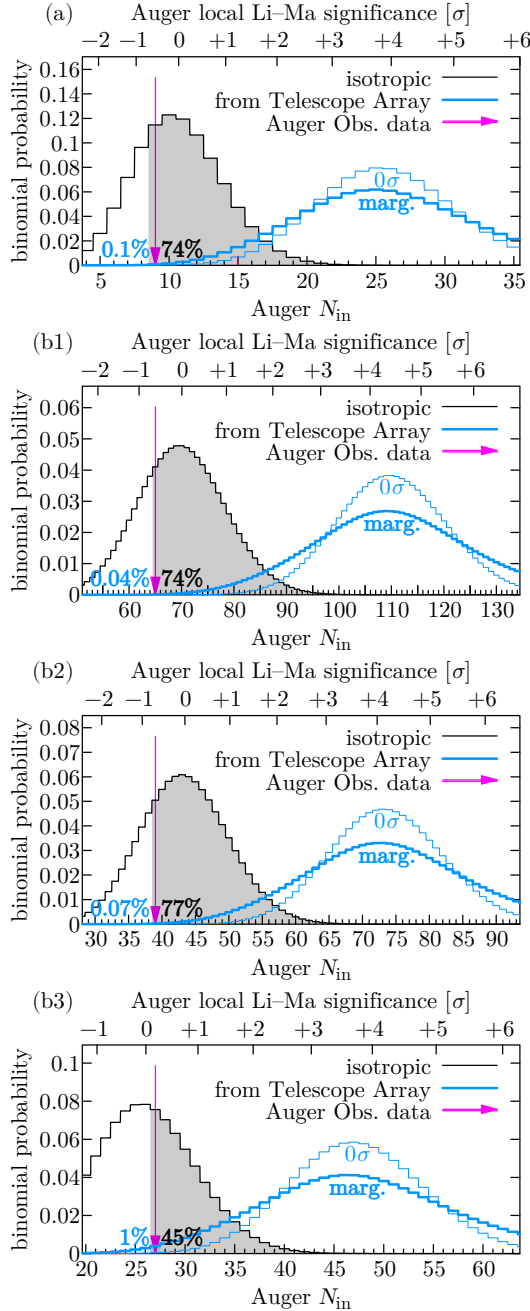


**Figure 4.** Binomial probability that  $N_{\text{in}}$  events would be observed in our dataset in each of the windows reported by TA and shown in Figure 3. The thin blue histogram assumes that the value of the flux ratio  $\Phi_{\text{in}}/\Phi_{\text{out}}$  is exactly the one reported by TA, whereas the thick one is the marginal distribution of  $\Phi_{\text{in}}/\Phi_{\text{out}}$  over TA statistical uncertainties.

the smaller statistics available back then. The growth of the strength  $\Phi_{\text{in}}/\Phi_{\text{out}}$  of the excess with increasing energy threshold could be explained if, for example, the excess originates from a single or a few nearby sources (whose identification would require accurately knowing the intervening magnetic deflections), whereas the back-

ground is from a large number of distant, more isotropically distributed sources. The steeper decrease with energy of the background would naturally be due to interactions with background photons in the intervening space (Greisen 1966; Zatsepin & Kuz'min 1966), as discussed in Pierre Auger Collaboration (2024).

On the other hand, no statistically significant excesses were found in the regions where TA reported excesses of events, despite comparable exposure. Given our current statistics, the Auger data do not support the suggestion of the Telescope Array Collaboration that the declination dependence of the UHECR energy spectrum, recently claimed by them in Telescope Array Collaboration (2024), is due to the presence of excesses in the flux of UHECRs from particular regions of the northern hemisphere.

It will be interesting to see whether the upgraded detectors of AugerPrime (Pierre Auger Collaboration 2016) and TA $\times$ 4 (Telescope Array Collaboration 2021a) and future experiments such as GRAND (GRAND Collaboration 2020), POEMMA (POEMMA Collaboration 2021) or GCOS (GCOS Collaboration 2023) will confirm or rule out the indications for excesses reported by current experiments, and/or detect other anisotropies too weak to be noticed with the number of events gathered so far by current observatories. If any excesses are confirmed, event-by-event mass information from upgraded detectors (Pierre Auger Collaboration 2016) and/or machine learning techniques (Pierre Auger Collaboration 2021a,b; Telescope Array Collaboration 2019) will help us elucidate their origin in the future by examining whether and how the mass composition in such regions differs from that in the rest of the sky and the energy dependence of any such differences.

#### ACKNOWLEDGMENTS

The successful installation, commissioning, and operation of the Pierre Auger Observatory would not have been possible without the strong commitment and effort from the technical and administrative staff in Malargüe. We are very grateful to the following agencies and organizations for financial support:

Argentina – Comisión Nacional de Energía Atómica; Agencia Nacional de Promoción Científica y Tecnológica (ANPCyT); Consejo Nacional de Investigaciones Científicas y Técnicas (CONICET); Gobierno de la Provincia de Mendoza; Municipalidad de Malargüe; NDM Holdings and Valle Las Leñas; in gratitude for their continuing cooperation over land access; Australia – the Australian Research Council; Belgium – Fonds de la Recherche Scientifique (FNRS); Research Foundation Flanders (FWO), Marie Curie Action of the European



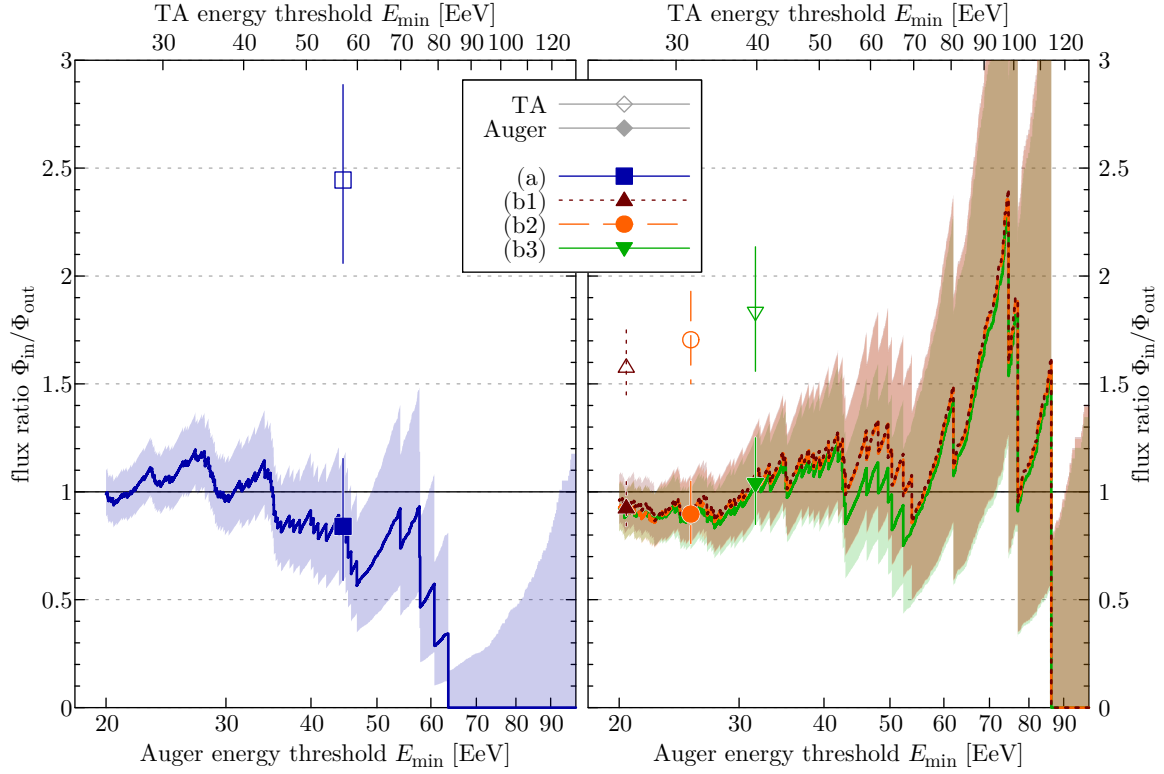


**Figure 5.** Flux ratio in the windows considered in this work (a, b1, b2, b3) computed from our data with all possible energy thresholds. The shaded bands show the  $\pm 1\sigma$  interval for each threshold. The filled markers indicate the values at the thresholds computed via [Pierre Auger Collaboration & Telescope Array Collaboration \(2023b, eq. \(1\)\)](#); the uncertainties on the energy cross-calibration are comparable to the horizontal size of the markers. The results reported in ([Telescope Array Collaboration 2023](#)) are also shown as empty markers for comparison.

Union Grant No. 101107047; Brazil – Conselho Nacional de Desenvolvimento Científico e Tecnológico (CNPq); Financiadora de Estudos e Projetos (FINEP); Fundação de Amparo à Pesquisa do Estado de Rio de Janeiro (FAPERJ); São Paulo Research Foundation (FAPESP) Grants No. 2019/10151-2, No. 2010/07359-6 and No. 1999/05404-3; Ministério da Ciência, Tecnologia, Inovações e Comunicações (MCTIC); Czech Republic – GACR 24-13049S, CAS LQ100102401, MEYS LM2023032, CZ.02.1.01/0.0/0.0/16\_013/0001402, CZ.02.1.01/0.0/0.0/18\_046/0016010 and CZ.02.1.01/0.0/0.0/17\_049/0008422 and CZ.02.01.01/00/22\_008/0004632; France – Centre de Calcul IN2P3/CNRS; Centre National de la Recherche Scientifique (CNRS); Conseil Régional Ile-de-France; Département Physique Nucléaire et Corpusculaire (PNC-IN2P3/CNRS); Département Sciences de l’Univers (SDU-INSU/CNRS); Institut Lagrange de Paris (ILP) Grant No. LABEX ANR-10-LABX-63 within the Investissements d’Avenir Programme Grant No. ANR-11-IDEX-0004-02; Germany – Bundesministerium für Bildung und Forschung (BMBF); Deutsche Forschungsgemeinschaft (DFG); Finanzministerium Baden-Württemberg; Helmholtz

Alliance for Astroparticle Physics (HAP); Helmholtz-Gemeinschaft Deutscher Forschungszentren (HGF); Ministerium für Kultur und Wissenschaft des Landes Nordrhein-Westfalen; Ministerium für Wissenschaft, Forschung und Kunst des Landes Baden-Württemberg; Italy – Istituto Nazionale di Fisica Nucleare (INFN); Istituto Nazionale di Astrofisica (INAF); Ministero dell’Università e della Ricerca (MUR); CETEMPS Center of Excellence; Ministero degli Affari Esteri (MAE), ICSC Centro Nazionale di Ricerca in High Performance Computing, Big Data and Quantum Computing, funded by European Union NextGenerationEU, reference code CN\_00000013; México – Consejo Nacional de Ciencia y Tecnología (CONACYT) No. 167733; Universidad Nacional Autónoma de México (UNAM); PAPIIT DGAPA-UNAM; The Netherlands – Ministry of Education, Culture and Science; Netherlands Organisation for Scientific Research (NWO); Dutch national e-infrastructure with the support of SURF Cooperative; Poland – Ministry of Education and Science, grants No. DIR/WK/2018/11 and 2022/WK/12; National Science Centre, grants No. 2016/22/M/ST9/00198, 2016/23/B/ST9/01635, 2020/39/B/ST9/01398, and 2022/45/B/ST9/02163; Portugal – Portuguese national

**Table 3.** Same as Table 1, but using a fixed window position  $(L, B) = (162^\circ, -6^\circ)$  and separate energy bins

$E_{\min}$	$E_{\max}$	$N_{\text{tot}}$	$N_{\text{bg}}$	$N_{\text{in}}$	$\frac{\Phi_{\text{in}}}{\Phi_{\text{out}}}$	$Z_{\text{LM}}$
20 EeV	25 EeV	3452	324.	389	$1.20^{+0.07}_{-0.06}$	$+3.3\sigma$
25 EeV	32 EeV	2444	233.	242	$1.04^{+0.07}_{-0.07}$	$+0.6\sigma$
32 EeV	40 EeV	1403	132.	151	$1.14^{+0.10}_{-0.10}$	$+1.5\sigma$
40 EeV	50 EeV	820	75.4	106	$1.41^{+0.15}_{-0.14}$	$+3.1\sigma$
50 EeV	63 EeV	418	37.9	59	$1.56^{+0.23}_{-0.21}$	$+3.0\sigma$
63 EeV	$+\infty$	295	26.6	43	$1.62^{+0.28}_{-0.25}$	$+2.7\sigma$

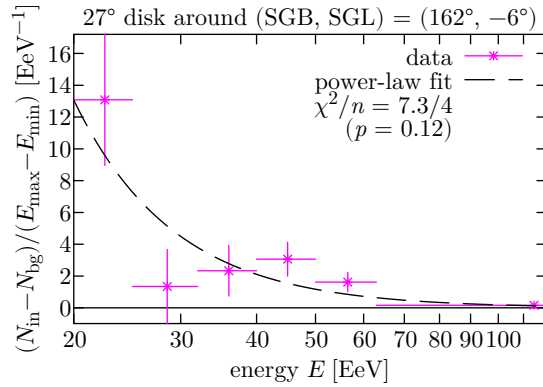


**Figure 6.** The number of excess events,  $N_{\text{in}} - N_{\text{bg}}$ , fitted as a power law spectrum  $N(E_{\min}, E_{\max}) = \int_{E_{\min}}^{E_{\max}} J_{20} \left( \frac{E}{20 \text{ EeV}} \right)^{-\gamma} dE = N_{20} \frac{E_{\min}^{1-\gamma} - E_{\max}^{1-\gamma}}{(20 \text{ EeV})^{1-\gamma}}$ . The uncertainty on each entry is the sum in quadrature of those on  $N_{\text{in}}$  and  $N_{\text{bg}}$ , computed as  $\sqrt{N_{\text{in}}}$  and  $\sqrt{N_{\text{out}} \mathcal{E}_{\text{in}} / \mathcal{E}_{\text{out}}}$  respectively. In the last bin, we use  $E_{\max} = 166 \text{ EeV}$ , the energy of the most energetic event. The best-fit parameter values we obtain are  $N_{20} = 160 \pm 32$  and  $\gamma = 2.63 \pm 0.35$ . Unlike in Pierre Auger Collaboration (2020b), in this work we do not correct for energy resolution effects; we estimate that here their effect on the spectral index would be an order of magnitude less than the statistical uncertainty of the fit.

funds and FEDER funds within Programa Operacional Factores de Competitividade through Fundação para a Ciência e a Tecnologia (COMPETE); Romania – Ministry of Research, Innovation and Digitization, CNCS-UEFISCDI, contract no. 30N/2023 under Romanian National Core Program LAPLAS VII, grant no. PN 23 21 01 02 and project number PN-III-P1-1.1-TE-2021-0924/TE57/2022, within PNCDI III; Slovenia – Slovenian Research Agency, grants P1-0031, P1-0385, I0-0033, N1-0111; Spain – Ministerio de Ciencia e Innovación/Agencia Estatal de Investigación (PID2019-105544GB-I00, PID2022-140510NB-I00 and

RYC2019-027017-I), Xunta de Galicia (CIGUS Network of Research Centers, Consolidación 2021 GRC GI-2033, ED431C-2021/22 and ED431F-2022/15), Junta de Andalucía (SOMM17/6104/UGR and P18-FR-4314), and the European Union (Marie Skłodowska-Curie 101065027 and ERDF); USA – Department of Energy, Contracts No. DE-AC02-07CH11359, No. DE-FR02-04ER41300, No. DE-FG02-99ER41107 and No. DE-SC0011689; National Science Foundation, Grant No. 0450696; The Grainger Foundation; Marie Curie-IRSES/EPLANET; European Particle Physics Latin American Network; and UNESCO.

## APPENDIX

### A. RESULTS USING SEPARATE ENERGY BINS

In order to describe the energy dependence of the excess in the Centaurus region, we also computed  $N_{\text{in}}$ ,  $N_{\text{bg}}$  and  $Z_{\text{LM}}$  in separate bins  $[20 \text{ EeV}, 25 \text{ EeV})$ ,  $\dots$ ,  $[50 \text{ EeV}, 63 \text{ EeV})$ ,  $[63 \text{ EeV}, +\infty)$  rather than cumulative ones  $[20 \text{ EeV}, +\infty)$ ,  $[25 \text{ EeV}, +\infty)$ ,  $\dots$ , keeping the window position fixed to the maximum-significance one found in  $[20 \text{ EeV}, +\infty)$ . The results are listed in Table 3. Also, we fitted a power-law energy spectrum  $\frac{dN}{dE} \propto E^{-\gamma}$  integrated over the bins to the excess  $N_{\text{in}} - N_{\text{bg}}$ , as shown in Figure 6. While the excess is considerably weaker in the third bin and barely present

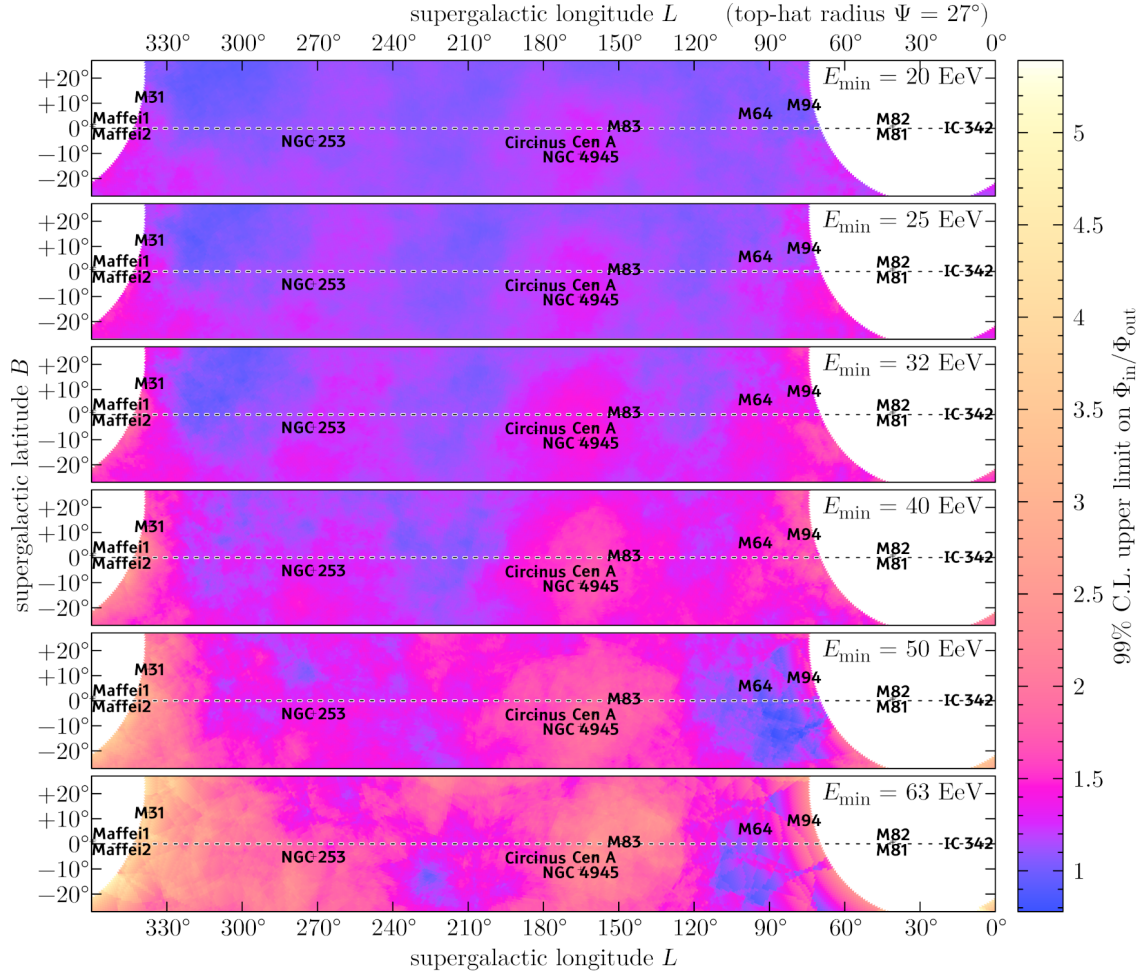


**Figure 7.** Same as Figure 1, showing the frequentist 99% CL upper limit to  $\Phi_{in}/\Phi_{out}$  (5)

in the second bin, the behavior is still consistent with a simple power law with the current amount of statistics.

## B. UPPER LIMITS AS A FUNCTION OF THE WINDOW POSITION

In Figure 7, we show the frequentist 99% CL upper limit to  $\Phi_{in}/\Phi_{out}$ , as determined from Equation 5 for each of the energy thresholds and window positions we considered, showing how our data can set stringent upper limits to the flux in the windows except very close to the edge of the FoV.

## REFERENCES

- Allard, D. 2012, *APh*, 39, 33
- Alves Batista, R., Shin, M.-S., Devriendt, J., Semikoz, D., & Sigl, G. 2017, *PhRvD*, 96, 023010
- Anchordoqui, L. A. 2023, *PhRvD*, 107, 083024
- GCOS Collaboration 2023, *PoS*, 444, 281, in Proc. 38th ICRC, 26 Jul.–3 Aug. 2023, Nagoya, Japan
- Górski, K. M., Hivon, E., Banday, A. J., Wandelt, B. D., Hansen, F. K., et al. 2005, *ApJ*, 622, 759
- GRAND Collaboration 2020, *SCPMA*, 63, 219501
- Greisen, K. 1966, *PhRvL*, 16, 748
- Lemoine, M., & Waxman, E. 2009, *JCAP*, 11, 009
- Li, T.-P., & Ma, Y.-Q. 1983, *ApJ*, 272, 317
- McCall, M. L. 2014, *MNRAS*, 440, 405
- Neronov, A., Semikoz, D., & Kalashev, O. 2023, *PhRvD*, 108, 103008
- Pierre Auger Collaboration 2010, *APh*, 34, 314
- Pierre Auger Collaboration 2011, *JCAP*, 06, 022
- Pierre Auger Collaboration 2016, [arXiv:1604.03637](https://arxiv.org/abs/1604.03637)

- Pierre Auger Collaboration 2017, *Sci*, 357, 1266
- Pierre Auger Collaboration 2018a, *ApJ*, 868, 4
- Pierre Auger Collaboration 2018b, *ApJL*, 853, L29
- Pierre Auger Collaboration 2020a, *ApJ*, 891, 142
- Pierre Auger Collaboration 2020b, *PhRvD*, 102, 062005
- Pierre Auger Collaboration 2021a, *JInst*, 16, P07016
- Pierre Auger Collaboration 2021b, *JInst*, 16, P07019
- Pierre Auger Collaboration 2022, *ApJ*, 935, 170 (data and code available at <https://doi.org/10.5281/zenodo.6504276>)
- Pierre Auger Collaboration 2023, *PoS*, 444, 252, in Proc. 38th ICRC, 26 Jul.–3 Aug. 2023, Nagoya, Japan
- Pierre Auger Collaboration 2024, *JCAP*, 01, 022
- Pierre Auger Collaboration & Telescope Array Collaboration 2021, *PoS*, 395, 308, in Proc. 37th ICRC, 12–23 Jul. 2021, Berlin, Germany
- Pierre Auger Collaboration & Telescope Array Collaboration 2023a, *EPJ Web Conf.*, 283, 03002, in Proc. 6th UHECR, 3–7 Oct. 2022, L’Aquila, Italy
- Pierre Auger Collaboration & Telescope Array Collaboration 2023b, *PoS*, 444, 521, in Proc. 38th ICRC, 26 Jul.–3 Aug. 2023, Nagoya, Japan
- Plotko, P., van Vliet, A., Rodrigues, X., & Winter, W. 2023, *ApJ*, 953, 129
- POEMMA Collaboration 2021, *JCAP*, 06, 007
- Pshirkov, M. S., Tinyakov, P. G., & Urban, F. U. 2013, *MNRAS*, 436, 2326
- Sommers, P. 2001, *Aph*, 14, 271
- Telescope Array Collaboration 2014, *ApJL*, 790, L21
- Telescope Array Collaboration 2018a, *ApJ*, 862, 91
- Telescope Array Collaboration 2018b, [arXiv:1801.07820](https://arxiv.org/abs/1801.07820)
- Telescope Array Collaboration 2019, *PhRvD*, 99, 022002
- Telescope Array Collaboration 2021a, *NIMPA*, 1019, 165726
- Telescope Array Collaboration 2021b, [arXiv:2110.14827](https://arxiv.org/abs/2110.14827)
- Telescope Array Collaboration 2023, *PoS*, 444, 244, in Proc. 38th ICRC, 26 Jul.–3 Aug. 2023, Nagoya, Japan
- Telescope Array Collaboration 2024, [arXiv:2406.08612](https://arxiv.org/abs/2406.08612)
- Unger, M., & Farrar, G. R. 2023, [arXiv:2311.12120](https://arxiv.org/abs/2311.12120)
- Zatsepin, G. T., & Kuz’min, V. A. 1966, *JETPL*, 4, 78

## The Pierre Auger Collaboration

A. Abdul Halim<sup>13</sup>, P. Abreu<sup>73</sup>, M. Aglietta<sup>55,53</sup>, I. Allekotte<sup>1</sup>, K. Almeida Cheminant<sup>71</sup>, A. Almela<sup>7,12</sup>, R. Aloisio<sup>46,47</sup>, J. Alvarez-Muñiz<sup>79</sup>, J. Ammerman Yebra<sup>79</sup>, G.A. Anastasi<sup>55,53</sup>, L. Anchordoqui<sup>86</sup>, B. Andrada<sup>7</sup>, S. Andringa<sup>73</sup>, Anukriti<sup>76</sup>, L. Apollonio<sup>60,50</sup>, C. Aramo<sup>51</sup>, P.R. Araújo Ferreira<sup>43</sup>, E. Arnone<sup>64,53</sup>, J.C. Arteaga Velázquez<sup>68</sup>, P. Assis<sup>73</sup>, G. Avila<sup>11</sup>, E. Avocone<sup>58,47</sup>, A. Bakalova<sup>33</sup>, F. Barbato<sup>46,47</sup>, A. Bartz Mocellin<sup>85</sup>, J.A. Bellido<sup>13,70</sup>, C. Berat<sup>37</sup>, M.E. Bertaina<sup>64,53</sup>, G. Bhatta<sup>71</sup>, M. Bianciotto<sup>64,53</sup>, P.L. Biermann<sup>i</sup>, V. Binet<sup>5</sup>, K. Bismark<sup>40,7</sup>, T. Bister<sup>80,81</sup>, J. Biteau<sup>38,b</sup>, J. Blazek<sup>33</sup>, C. Bleve<sup>37</sup>, J. Blümer<sup>42</sup>, M. Boháčová<sup>33</sup>, D. Boncioli<sup>58,47</sup>, C. Bonifazi<sup>8,27</sup>, L. Bonneau Arbeletche<sup>22</sup>, N. Borodai<sup>71</sup>, J. Brack<sup>k</sup>, P.G. Brichetto Orcherá<sup>7</sup>, F.L. Briechele<sup>43</sup>, A. Bueno<sup>78</sup>, S. Buitink<sup>15</sup>, M. Buscemi<sup>48,62</sup>, M. Büsken<sup>40,7</sup>, A. Bwembya<sup>80,81</sup>, K.S. Caballero-Mora<sup>67</sup>, S. Cabana-Freire<sup>79</sup>, L. Caccianiga<sup>60,50</sup>, R. Caruso<sup>59,48</sup>, A. Castellina<sup>55,53</sup>, F. Catalani<sup>19</sup>, G. Cataldi<sup>49</sup>, L. Cazon<sup>79</sup>, M. Cerda<sup>10</sup>, A. Cermenati<sup>46,47</sup>, J.A. Chinellato<sup>22</sup>, J. Chudoba<sup>33</sup>, L. Chytka<sup>34</sup>, R.W. Clay<sup>13</sup>, A.C. Cobos Cerutti<sup>6</sup>, R. Colalillo<sup>61,51</sup>, A. Coleman<sup>90</sup>, M.R. Coluccia<sup>49</sup>, R. Conceição<sup>73</sup>, A. Condorelli<sup>38</sup>, G. Consolati<sup>50,56</sup>, M. Conte<sup>57,49</sup>, F. Convenga<sup>58,47</sup>, D. Correia dos Santos<sup>29</sup>, P.J. Costa<sup>73</sup>, C.E. Covault<sup>84</sup>, M. Cristinziani<sup>45</sup>, C.S. Cruz Sanchez<sup>3</sup>, S. Dasso<sup>4,2</sup>, K. Daumiller<sup>42</sup>, B.R. Dawson<sup>13</sup>, R.M. de Almeida<sup>29</sup>, J. de Jesús<sup>7,42</sup>, S.J. de Jong<sup>80,81</sup>, J.R.T. de Mello Neto<sup>27,28</sup>, I. De Mitri<sup>46,47</sup>, J. de Oliveira<sup>18</sup>, D. de Oliveira Franco<sup>22</sup>, F. de Palma<sup>57,49</sup>, V. de Souza<sup>20</sup>, B.P. de Souza de Errico<sup>27</sup>, E. De Vito<sup>57,49</sup>, A. Del Popolo<sup>59,48</sup>, O. Deligny<sup>35</sup>, N. Denner<sup>33</sup>, L. Deval<sup>42,7</sup>, A. di Matteo<sup>53</sup>, M. Dobre<sup>74</sup>, C. Dobrigkeit<sup>22</sup>, J.C. D’Olivo<sup>69</sup>, L.M. Domingues Mendes<sup>73</sup>, Q. Dorosti<sup>45</sup>, J.C. dos Anjos<sup>16</sup>, R.C. dos Anjos<sup>26</sup>, J. Ebr<sup>33</sup>, F. Ellwanger<sup>42</sup>, M. Emam<sup>80,81</sup>, R. Engel<sup>40,42</sup>, I. Epicoco<sup>57,49</sup>, M. Erdmann<sup>43</sup>, A. Etchegoyen<sup>7,12</sup>, C. Evoli<sup>46,47</sup>, H. Falcke<sup>80,82,81</sup>, J. Farmer<sup>89</sup>, G. Farrar<sup>88</sup>, A.C. Fauth<sup>22</sup>, N. Fazzini<sup>f</sup>, F. Feldbusch<sup>41</sup>, F. Fenu<sup>42,e</sup>, A. Fernandes<sup>73</sup>, B. Fick<sup>87</sup>, J.M. Figueira<sup>7</sup>, A. Filipčić<sup>77,76</sup>, T. Fitoussi<sup>42</sup>, B. Flaggs<sup>90</sup>, T. Fodran<sup>80</sup>, T. Fujii<sup>89,g</sup>, A. Fuster<sup>7,12</sup>, C. Galea<sup>80</sup>, C. Galelli<sup>60,50</sup>, B. García<sup>6</sup>, C. Gaudu<sup>39</sup>, H. Gemmeke<sup>41</sup>, F. Gesualdi<sup>7,42</sup>, A. Gherghel-Lascu<sup>74</sup>, P.L. Ghia<sup>35</sup>, U. Giaccari<sup>49</sup>, J. Glombitza<sup>43,h</sup>, F. Gobbi<sup>10</sup>, F. Gollan<sup>7</sup>, G. Golup<sup>1</sup>, M. Gómez Berisso<sup>1</sup>, P.F. Gómez Vitale<sup>11</sup>, J.P. Gongora<sup>11</sup>, J.M. González<sup>1</sup>, N. González<sup>7</sup>, I. Goos<sup>1</sup>, D. Góra<sup>71</sup>, A. Gorgi<sup>55,53</sup>, M. Gottowik<sup>79</sup>, T.D. Grubb<sup>13</sup>, F. Guarino<sup>61,51</sup>, G.P. Guedes<sup>23</sup>, E. Guido<sup>45</sup>, L. Gülzow<sup>42</sup>, S. Hahn<sup>40</sup>, P. Hamal<sup>33</sup>, M.R. Hampel<sup>7</sup>, P. Hansen<sup>3</sup>, D. Harari<sup>1</sup>, V.M. Harvey<sup>13</sup>, A. Haungs<sup>42</sup>, T. Hebbeker<sup>43</sup>, C. Hojvat<sup>f</sup>, J.R. Hörandel<sup>80,81</sup>, P. Horvath<sup>34</sup>, M. Hrabovský<sup>34</sup>, T. Huege<sup>42,15</sup>, A. Insolia<sup>59,48</sup>, P.G. Isar<sup>75</sup>, P. Janecek<sup>33</sup>, V. Jilek<sup>33</sup>, J.A. Johnsen<sup>85</sup>, J. Jurysek<sup>33</sup>, K.-H. Kampert<sup>39</sup>, B. Keilhauer<sup>42</sup>, A. Khakurdikar<sup>80</sup>, V.V. Kizakke Covilakam<sup>7,42</sup>, H.O. Klages<sup>42</sup>, M. Kleifges<sup>41</sup>, F. Knapp<sup>40</sup>, J. Köhler<sup>42</sup>, N. Kunka<sup>41</sup>, B.L. Lago<sup>17</sup>, N. Langner<sup>43</sup>, M.A. Leigui de Oliveira<sup>25</sup>, Y. Lema-Capeans<sup>79</sup>, A. Letessier-Selvon<sup>36</sup>, I. Lhenry-Yvon<sup>35</sup>, L. Lopes<sup>73</sup>, L. Lu<sup>91</sup>, Q. Luce<sup>40</sup>, J.P. Lundquist<sup>76</sup>, A. Machado Payeras<sup>22</sup>, M. Majercakova<sup>33</sup>, D. Mandat<sup>33</sup>, B.C. Manning<sup>13</sup>, P. Mantsch<sup>f</sup>, S. Marafico<sup>35</sup>, F.M. Mariani<sup>60,50</sup>, A.G. Mariazzi<sup>3</sup>, I.C. Mariş<sup>14</sup>, G. Marsella<sup>62,48</sup>, D. Martello<sup>57,49</sup>, S. Martinelli<sup>42,7</sup>, O. Martínez Bravo<sup>65</sup>, M.A. Martins<sup>79</sup>, H.-J. Mathes<sup>42</sup>, J. Matthews<sup>a</sup>, G. Matthiae<sup>63,52</sup>, E. Mayotte<sup>85,39</sup>, S. Mayotte<sup>85</sup>, P.O. Mazur<sup>f</sup>, G. Medina-Tanco<sup>69</sup>, J. Meinert<sup>39</sup>, D. Melo<sup>7</sup>, A. Menshikov<sup>41</sup>, C. Merx<sup>42</sup>, S. Michal<sup>34</sup>, M.I. Micheletti<sup>5</sup>, L. Miramonti<sup>60,50</sup>, S. Mollerach<sup>1</sup>, F. Montanet<sup>37</sup>, L. Morejon<sup>39</sup>, C. Morello<sup>55,53</sup>, K. Mulrey<sup>80,81</sup>, R. Mussa<sup>53</sup>, W.M. Namasaka<sup>39</sup>, S. Negi<sup>33</sup>, L. Nellen<sup>69</sup>, K. Nguyen<sup>87</sup>, G. Nicora<sup>9</sup>, M. Niechciol<sup>45</sup>, D. Nitz<sup>87</sup>, D. Nosek<sup>32</sup>, V. Novotny<sup>32</sup>, L. Nožka<sup>34</sup>, A. Nucita<sup>57,49</sup>, L.A. Núñez<sup>31</sup>, C. Oliveira<sup>20</sup>, M. Palatka<sup>33</sup>, J. Pallotta<sup>9</sup>, S. Panja<sup>33</sup>, G. Parente<sup>79</sup>, T. Paulsen<sup>39</sup>, J. Pawlowsky<sup>39</sup>, M. Pech<sup>33</sup>, J. Pękala<sup>71</sup>, R. Pelayo<sup>66</sup>, L.A.S. Pereira<sup>24</sup>, E.E. Pereira Martins<sup>40,7</sup>, J. Perez Armand<sup>21</sup>, C. Pérez Bertoli<sup>7,42</sup>, L. Perrone<sup>57,49</sup>, S. Petrerá<sup>46,47</sup>, C. Petrucci<sup>58,47</sup>, T. Pierog<sup>42</sup>, M. Pimenta<sup>73</sup>, M. Platino<sup>7</sup>, B. Pont<sup>80</sup>, M. Pothast<sup>81,80</sup>, M. Pourmohammad Shahvar<sup>62,48</sup>, P. Privitera<sup>89</sup>, M. Prouza<sup>33</sup>, A. Puyleart<sup>87</sup>, S. Querchfeld<sup>39</sup>, J. Rautenberg<sup>39</sup>, D. Ravignani<sup>7</sup>, J.V. Reginatto Akim<sup>22</sup>, M. Reininghaus<sup>40</sup>, J. Ridky<sup>33</sup>, F. Riehn<sup>79</sup>, M. Risse<sup>45</sup>, V. Rizi<sup>58,47</sup>, W. Rodrigues de Carvalho<sup>80</sup>, E. Rodriguez<sup>7,42</sup>, J. Rodriguez Rojo<sup>11</sup>, M.J. Roncoroni<sup>7</sup>, S. Rossoni<sup>44</sup>, M. Roth<sup>42</sup>, E. Roulet<sup>1</sup>, A.C. Rovero<sup>4</sup>, P. Ruehl<sup>45</sup>, A. Saftoiu<sup>74</sup>, M. Saharan<sup>80</sup>, F. Salamida<sup>58,47</sup>, H. Salazar<sup>65</sup>, G. Salina<sup>52</sup>, J.D. Sanabria Gomez<sup>31</sup>, F. Sánchez<sup>7</sup>, E.M. Santos<sup>21</sup>, E. Santos<sup>33</sup>, F. Sarazin<sup>85</sup>, R. Sarmiento<sup>73</sup>, R. Sato<sup>11</sup>, P. Savina<sup>91</sup>, C.M. Schäfer<sup>40</sup>, V. Scherini<sup>57,49</sup>, H. Schieler<sup>42</sup>, M. Schimassek<sup>35</sup>, M. Schimp<sup>39</sup>, D. Schmidt<sup>42</sup>, O. Scholten<sup>15,j</sup>, H. Schoorlemmer<sup>80,81</sup>, P. Schovánek<sup>33</sup>, F.G. Schröder<sup>90,42</sup>, J. Schulte<sup>43</sup>, T. Schulz<sup>42</sup>, S.J. Sciutto<sup>3</sup>, M. Scornavacche<sup>7,42</sup>, A. Segreto<sup>54,48</sup>, S. Sehgal<sup>39</sup>, S.U. Shivashankara<sup>76</sup>, G. Sigl<sup>44</sup>, G. Silli<sup>7</sup>, O. Sima<sup>74,c</sup>, K. Simkova<sup>15</sup>, F. Simon<sup>41</sup>, R. Smau<sup>74</sup>, R. Šmída<sup>89</sup>, P. Sommers<sup>l</sup>, J.F. Soriano<sup>86</sup>, R. Squartini<sup>10</sup>, M. Stadelmaier<sup>50,60,42</sup>, S. Stanič<sup>76</sup>, J. Stasielak<sup>71</sup>, P. Stassi<sup>37</sup>, S. Strähnz<sup>40</sup>, M. Straub<sup>43</sup>, T. Suomijärvi<sup>38</sup>, A.D. Supanitsky<sup>7</sup>, Z. Svozilikova<sup>33</sup>, Z. Szadkowski<sup>72</sup>, F. Tairli<sup>13</sup>, A. Tapia<sup>30</sup>, C. Taricco<sup>64,53</sup>, C. Timmermans<sup>81,80</sup>, O. Tkachenko<sup>42</sup>, P. Tobiska<sup>33</sup>, C.J. Todero Peixoto<sup>19</sup>, B. Tomé<sup>73</sup>, Z. Torrès<sup>37</sup>, A. Travaini<sup>10</sup>, P. Travnicek<sup>33</sup>, C. Trimarelli<sup>58,47</sup>, M. Tueros<sup>3</sup>, M. Unger<sup>42</sup>, L. Vaclavěk<sup>34</sup>, M. Vacula<sup>34</sup>, J.F. Valdés Galicia<sup>69</sup>, L. Valore<sup>61,51</sup>, E. Varela<sup>65</sup>, A. Vásquez-Ramírez<sup>31</sup>, D. Veberič<sup>42</sup>, C. Ventura<sup>28</sup>, I.D. Vergara Quispe<sup>3</sup>, V. Verzi<sup>52</sup>, J. Vicha<sup>33</sup>, J. Vink<sup>83</sup>, S. Vorobiov<sup>76</sup>, C. Watanabe<sup>27</sup>, A.A. Watson<sup>d</sup>, A. Weindl<sup>42</sup>,

L. Wiencke<sup>85</sup>, H. Wilczyński<sup>71</sup>, D. Wittkowski<sup>39</sup>, B. Wundheiler<sup>7</sup>, B. Yue<sup>39</sup>, A. Yushkov<sup>33</sup>, O. Zapparrata<sup>14</sup>, E. Zas<sup>79</sup>, D. Zavrtanik<sup>76,77</sup>, M. Zavrtanik<sup>77,76</sup>

- <sup>1</sup> Centro Atómico Bariloche and Instituto Balseiro (CNEA-UNCuyo-CONICET), San Carlos de Bariloche, Argentina
- <sup>2</sup> Departamento de Física and Departamento de Ciencias de la Atmósfera y los Océanos, FCEyN, Universidad de Buenos Aires and CONICET, Buenos Aires, Argentina
- <sup>3</sup> IFLP, Universidad Nacional de La Plata and CONICET, La Plata, Argentina
- <sup>4</sup> Instituto de Astronomía y Física del Espacio (IAFE, CONICET-UBA), Buenos Aires, Argentina
- <sup>5</sup> Instituto de Física de Rosario (IFIR) – CONICET/U.N.R. and Facultad de Ciencias Bioquímicas y Farmacéuticas U.N.R., Rosario, Argentina
- <sup>6</sup> Instituto de Tecnologías en Detección y Astropartículas (CNEA, CONICET, UNSAM), and Universidad Tecnológica Nacional – Facultad Regional Mendoza (CONICET/CNEA), Mendoza, Argentina
- <sup>7</sup> Instituto de Tecnologías en Detección y Astropartículas (CNEA, CONICET, UNSAM), Buenos Aires, Argentina
- <sup>8</sup> International Center of Advanced Studies and Instituto de Ciencias Físicas, ECyT-UNSAM and CONICET, Campus Miguelete – San Martín, Buenos Aires, Argentina
- <sup>9</sup> Laboratorio Atmósfera – Departamento de Investigaciones en Láseres y sus Aplicaciones – UNIDEF (CITEDEF-CONICET), Argentina
- <sup>10</sup> Observatorio Pierre Auger, Malargüe, Argentina
- <sup>11</sup> Observatorio Pierre Auger and Comisión Nacional de Energía Atómica, Malargüe, Argentina
- <sup>12</sup> Universidad Tecnológica Nacional – Facultad Regional Buenos Aires, Buenos Aires, Argentina
- <sup>13</sup> University of Adelaide, Adelaide, S.A., Australia
- <sup>14</sup> Université Libre de Bruxelles (ULB), Brussels, Belgium
- <sup>15</sup> Vrije Universiteit Brussels, Brussels, Belgium
- <sup>16</sup> Centro Brasileiro de Pesquisas Físicas, Rio de Janeiro, RJ, Brazil
- <sup>17</sup> Centro Federal de Educação Tecnológica Celso Suckow da Fonseca, Petropolis, Brazil
- <sup>18</sup> Instituto Federal de Educação, Ciência e Tecnologia do Rio de Janeiro (IFRJ), Brazil
- <sup>19</sup> Universidade de São Paulo, Escola de Engenharia de Lorena, Lorena, SP, Brazil
- <sup>20</sup> Universidade de São Paulo, Instituto de Física de São Carlos, São Carlos, SP, Brazil
- <sup>21</sup> Universidade de São Paulo, Instituto de Física, São Paulo, SP, Brazil
- <sup>22</sup> Universidade Estadual de Campinas, IFGW, Campinas, SP, Brazil
- <sup>23</sup> Universidade Estadual de Feira de Santana, Feira de Santana, Brazil
- <sup>24</sup> Universidade Federal de Campina Grande, Centro de Ciências e Tecnologia, Campina Grande, Brazil
- <sup>25</sup> Universidade Federal do ABC, Santo André, SP, Brazil
- <sup>26</sup> Universidade Federal do Paraná, Setor Palotina, Palotina, Brazil
- <sup>27</sup> Universidade Federal do Rio de Janeiro, Instituto de Física, Rio de Janeiro, RJ, Brazil
- <sup>28</sup> Universidade Federal do Rio de Janeiro (UFRJ), Observatório do Valongo, Rio de Janeiro, RJ, Brazil
- <sup>29</sup> Universidade Federal Fluminense, EEIMVR, Volta Redonda, RJ, Brazil
- <sup>30</sup> Universidad de Medellín, Medellín, Colombia
- <sup>31</sup> Universidad Industrial de Santander, Bucaramanga, Colombia
- <sup>32</sup> Charles University, Faculty of Mathematics and Physics, Institute of Particle and Nuclear Physics, Prague, Czech Republic
- <sup>33</sup> Institute of Physics of the Czech Academy of Sciences, Prague, Czech Republic
- <sup>34</sup> Palacky University, Olomouc, Czech Republic
- <sup>35</sup> CNRS/IN2P3, IJCLab, Université Paris-Saclay, Orsay, France
- <sup>36</sup> Laboratoire de Physique Nucléaire et de Hautes Energies (LPNHE), Sorbonne Université, Université de Paris, CNRS-IN2P3, Paris, France
- <sup>37</sup> Univ. Grenoble Alpes, CNRS, Grenoble Institute of Engineering Univ. Grenoble Alpes, LPSC-IN2P3, 38000 Grenoble, France
- <sup>38</sup> Université Paris-Saclay, CNRS/IN2P3, IJCLab, Orsay, France
- <sup>39</sup> Bergische Universität Wuppertal, Department of Physics, Wuppertal, Germany
- <sup>40</sup> Karlsruhe Institute of Technology (KIT), Institute for Experimental Particle Physics, Karlsruhe, Germany
- <sup>41</sup> Karlsruhe Institute of Technology (KIT), Institut für Prozessdatenverarbeitung und Elektronik, Karlsruhe, Germany
- <sup>42</sup> Karlsruhe Institute of Technology (KIT), Institute for Astroparticle Physics, Karlsruhe, Germany

- <sup>43</sup> RWTH Aachen University, III. Physikalisches Institut A, Aachen, Germany
- <sup>44</sup> Universität Hamburg, II. Institut für Theoretische Physik, Hamburg, Germany
- <sup>45</sup> Universität Siegen, Department Physik – Experimentelle Teilchenphysik, Siegen, Germany
- <sup>46</sup> Gran Sasso Science Institute, L’Aquila, Italy
- <sup>47</sup> INFN Laboratori Nazionali del Gran Sasso, Assergi (L’Aquila), Italy
- <sup>48</sup> INFN, Sezione di Catania, Catania, Italy
- <sup>49</sup> INFN, Sezione di Lecce, Lecce, Italy
- <sup>50</sup> INFN, Sezione di Milano, Milano, Italy
- <sup>51</sup> INFN, Sezione di Napoli, Napoli, Italy
- <sup>52</sup> INFN, Sezione di Roma “Tor Vergata”, Roma, Italy
- <sup>53</sup> INFN, Sezione di Torino, Torino, Italy
- <sup>54</sup> Istituto di Astrofisica Spaziale e Fisica Cosmica di Palermo (INAF), Palermo, Italy
- <sup>55</sup> Osservatorio Astrofisico di Torino (INAF), Torino, Italy
- <sup>56</sup> Politecnico di Milano, Dipartimento di Scienze e Tecnologie Aerospaziali, Milano, Italy
- <sup>57</sup> Università del Salento, Dipartimento di Matematica e Fisica “E. De Giorgi”, Lecce, Italy
- <sup>58</sup> Università dell’Aquila, Dipartimento di Scienze Fisiche e Chimiche, L’Aquila, Italy
- <sup>59</sup> Università di Catania, Dipartimento di Fisica e Astronomia “Ettore Majorana”, Catania, Italy
- <sup>60</sup> Università di Milano, Dipartimento di Fisica, Milano, Italy
- <sup>61</sup> Università di Napoli “Federico II”, Dipartimento di Fisica “Ettore Pancini”, Napoli, Italy
- <sup>62</sup> Università di Palermo, Dipartimento di Fisica e Chimica “E. Segrè”, Palermo, Italy
- <sup>63</sup> Università di Roma “Tor Vergata”, Dipartimento di Fisica, Roma, Italy
- <sup>64</sup> Università Torino, Dipartimento di Fisica, Torino, Italy
- <sup>65</sup> Benemérita Universidad Autónoma de Puebla, Puebla, México
- <sup>66</sup> Unidad Profesional Interdisciplinaria en Ingeniería y Tecnologías Avanzadas del Instituto Politécnico Nacional (UPIITA-IPN), México, D.F., México
- <sup>67</sup> Universidad Autónoma de Chiapas, Tuxtla Gutiérrez, Chiapas, México
- <sup>68</sup> Universidad Michoacana de San Nicolás de Hidalgo, Morelia, Michoacán, México
- <sup>69</sup> Universidad Nacional Autónoma de México, México, D.F., México
- <sup>70</sup> Universidad Nacional de San Agustín de Arequipa, Facultad de Ciencias Naturales y Formales, Arequipa, Peru
- <sup>71</sup> Institute of Nuclear Physics PAN, Krakow, Poland
- <sup>72</sup> University of Łódź, Faculty of High-Energy Astrophysics, Łódź, Poland
- <sup>73</sup> Laboratório de Instrumentação e Física Experimental de Partículas – LIP and Instituto Superior Técnico – IST, Universidade de Lisboa – UL, Lisboa, Portugal
- <sup>74</sup> “Horia Hulubei” National Institute for Physics and Nuclear Engineering, Bucharest-Magurele, Romania
- <sup>75</sup> Institute of Space Science, Bucharest-Magurele, Romania
- <sup>76</sup> Center for Astrophysics and Cosmology (CAC), University of Nova Gorica, Nova Gorica, Slovenia
- <sup>77</sup> Experimental Particle Physics Department, J. Stefan Institute, Ljubljana, Slovenia
- <sup>78</sup> Universidad de Granada and C.A.F.P.E., Granada, Spain
- <sup>79</sup> Instituto Galego de Física de Altas Enerxías (IGFAE), Universidade de Santiago de Compostela, Santiago de Compostela, Spain
- <sup>80</sup> IMAPP, Radboud University Nijmegen, Nijmegen, The Netherlands
- <sup>81</sup> Nationaal Instituut voor Kernfysica en Hoge Energie Fysica (NIKHEF), Science Park, Amsterdam, The Netherlands
- <sup>82</sup> Stichting Astronomisch Onderzoek in Nederland (ASTRON), Dwingeloo, The Netherlands
- <sup>83</sup> Universiteit van Amsterdam, Faculty of Science, Amsterdam, The Netherlands
- <sup>84</sup> Case Western Reserve University, Cleveland, OH, USA
- <sup>85</sup> Colorado School of Mines, Golden, CO, USA
- <sup>86</sup> Department of Physics and Astronomy, Lehman College, City University of New York, Bronx, NY, USA
- <sup>87</sup> Michigan Technological University, Houghton, MI, USA
- <sup>88</sup> New York University, New York, NY, USA
- <sup>89</sup> University of Chicago, Enrico Fermi Institute, Chicago, IL, USA
- <sup>90</sup> University of Delaware, Department of Physics and Astronomy, Bartol Research Institute, Newark, DE, USA
- <sup>91</sup> University of Wisconsin-Madison, Department of Physics and WIPAC, Madison, WI, USA

---

<sup>a</sup> Louisiana State University, Baton Rouge, LA, USA

<sup>b</sup> Institut universitaire de France (IUF), France

<sup>c</sup> also at University of Bucharest, Physics Department, Bucharest, Romania

<sup>d</sup> School of Physics and Astronomy, University of Leeds, Leeds, United Kingdom

<sup>e</sup> now at Agenzia Spaziale Italiana (ASI). Via del Politecnico 00133, Roma, Italy

<sup>f</sup> Fermi National Accelerator Laboratory, Fermilab, Batavia, IL, USA

<sup>g</sup> now at Graduate School of Science, Osaka Metropolitan University, Osaka, Japan

<sup>h</sup> now at ECAP, Erlangen, Germany

<sup>i</sup> Max-Planck-Institut für Radioastronomie, Bonn, Germany

<sup>j</sup> also at Kapteyn Institute, University of Groningen, Groningen, The Netherlands

<sup>k</sup> Colorado State University, Fort Collins, CO, USA

<sup>l</sup> Pennsylvania State University, University Park, PA, USA